



Crystallization Behavior and Properties of Hypereutectic Al-Si Alloys with Different Iron Content

V. Deev^{a,b}, E. Prusov^{c*}, O. Prikhodko^d, E. Ri^e, A. Kutsenko^d, S. Smetanyuk^f

^aWuhan Textile University, China

^bNational University of Science and Technology «MISIS», Russia

^cVladimir State University named after Alexander and Nikolay Stoletovs, Russia

^dSiberian State Industrial University, Russia

^ePacific National University, Russia

^fSiberian Federal University, Russia

* Corresponding author. E-mail address: eprusov@mail.ru

Received 10.07.2020; accepted in revised form 22.10.2020

Abstract

Understanding the influence of iron impurity on the formation of the structure and the properties of hypereutectic aluminum-silicon alloys are important for achieving the required quality of castings, especially those obtained from secondary materials. In the present work, the influence of different iron contents (0.3, 1.1, and 2.0 wt.%) on the crystallization process, microstructure and mechanical properties of the Al-15% Si alloy was studied. It is shown that the presence of iron impurity in the Al-15% Si alloy leads to increasing the eutectic crystallization time from 6.2 to 7.6 s at increasing the iron content from 0.3 wt.% to 1.1 wt.%, changing the structure of the alloy eutectic in the solid state. The primary silicon and β -Al₃SiFe phase coexist in the structure of the Al-15% Si alloys at a temperature below 575 °C in the range of iron concentrations from 0 to 2 wt.% in equilibrium conditions. In the experimental alloys structure, the primary crystals of the β -phase were metallographically detected only in the alloys containing 1.1 and 2 wt.% of iron impurity. Increase of the iron content up to 2 wt.% significantly reduces the mechanical properties of the Al-15% Si alloy due to the formation of large platelet-like inclusions of β -Al₃SiFe phase.

Keywords: Hypereutectic aluminium-silicon alloys, Iron-rich compounds, Intermetallics, Crystallization, Mechanical properties

1. Introduction

The problem of contamination of the initial charging materials with harmful residual elements, primarily iron, draws the relentless focus of researchers and manufacturers [1-4]. Due to its very low solubility in solid aluminum (max. 0.05 wt.%), the iron impurity in aluminum alloys promotes the formation of various intermetallic phases with coarse-grained structure, which

substantially reduces the quality of the castings [5]. Many issues related to the effect of iron on the structure and properties of Al-Si alloys have been underinvestigated up to date. It especially concerns hypereutectic Al-Si alloys [6]. Depending on its state, iron in such alloys can have both negative and positive effects, in second case allowing to improve the high-temperature properties and thermal stability of the alloy [7]. In turn, the negative effect of iron can manifest itself in a significant decrease in tensile

strength, ductility, toughness, corrosion resistance and other properties [8, 9].

In the Al-Si-Fe system, phases of different composition and morphology can be formed depending on the Fe/Si ratio in the alloy [10]. At small iron content (less than 0.8 wt.%) in low-silicon Al-Si alloys, the iron-containing phase falls out as a chemical compound $\text{Al}_8\text{Fe}_2\text{Si}$ (α) crystallizing in the form of skeleton-like crystals ("Chinese script"). The Al_5FeSi (β) phase is formed with an increase of silicon and iron content. The primary crystals of this phase have a plate-like shape (needle-like in the plane of the 2D section) [11, 12]. The Al_4FeSi_2 (δ) phase is often exist in silicon-rich alloys (> 14 wt.% Si); the Al_3FeSi (γ) phase is observed in alloys rich in iron (> 6 wt.% Fe) and silicon (> 14 wt.% Si) [13]. Along with the alloy chemical composition, the morphology of intermetallic compounds in iron-containing Al-Si alloys significantly depend on the conditions of the castings solidification [14], and also on the conditions of the melt treatment [15].

The main structural constituents of hypereutectic Al-Si alloys are aluminum dendrites (α -solid solution), eutectic (α -Al + Si) and primary silicon crystals [16]. The iron-containing α -phase ($\text{Al}_8\text{Fe}_2\text{Si}$) is practically not formed in industrial aluminum-silicon alloys. Iron at concentrations 0.5...0.8 wt.% is usually fixed into the eutectic (β + α -Al + Si) in the form of thin plates distributed among silicon needles and cores. During the crystallization of this eutectic, the β -phase (Al_5FeSi) is the leading one, and the growth of silicon crystals together with aluminum starts from it. If the amount of iron exceeds 0.8%, Al_5FeSi primary crystals appear [17]. It should be noted that brittle β -phase (Al_5FeSi) is an undesirable constituent of the Al-Si alloy structure, since cracks are easily formed on the sharp edges of the needle crystals, and then propagate along its entire length [18]. A high fraction of iron-containing β -phase in aluminum alloys also leads to a decrease in the fluidity of the melts [19].

Hypereutectic aluminum-silicon alloys can be considered as natural in-situ composites where the particles of primary silicon play the role of the endogenous reinforcing phase [20]. In this connection, it is expedient to analyze the influence of impurity elements on the change of the structural and morphological characteristics of hypereutectic Al-Si alloy and their technological and operational properties with account of cast metal matrix composites behavior [21]. The presence of primary silicon particles in the eutectic matrix causes high wear resistance, thermal stability, and low coefficient of thermal expansion [22]. In this case, a combination of good casting and mechanical properties is possible in hypereutectic Al-Si alloys with a relatively low silicon content, for example, Al-15% Si [23]. Such combination of properties makes these alloys promising for manufacturing of shaped castings with complex configuration for automotive and aerospace applications (engine blocks, pistons, etc.). In particular, the Al-15% Si system is the basis of the industrial alloy A390, which serves as one of the common piston materials [24]. Taking into account the modern trends in increasing the amount of the secondary alloys using for castings manufacturing (including hypereutectic Al-Si alloys), it is important to estimate the effect of iron impurity on the processes of structure formation and properties of cast parts.

In recent studies devoted to hypereutectic Al-Si alloys, the main attention has been focused on modifying the Fe-rich

intermetallic compounds to reduce its harmful effect. In particular, it was reported that the addition of 0.6 wt.% Mn to the hypereutectic alloy Al-17.5%Si-1.2%Fe changed the beta intermetallics into the modified alpha phases [25]. On an example of the Al-14Si-2Fe alloy (wt.%), it was shown that the application of pressure up to 300 MPa during rheo-squeeze casting can significantly reduce the size and improve the morphology of Fe-rich phases [26]. Changes in the structure and mechanical properties of alloys are possible by various energetic influences (for example, electron-beam treatment), leading to a significant increase in the fatigue life of the samples [27]. However, information on the crystallization behavior of hypereutectic Al-Si alloys in the presence of an iron impurity is limited.

The aim of this work is to study the effect of different iron contents (0.3, 1.1, and 2.0 wt.%) on the crystallization process, microstructure and properties of the Al-15% Si alloy.

2. Materials and Methods

Pure components was used for the obtaining of experimental alloys: aluminum (> 99.99 wt.% Al), silicon (> 99.0 wt.% Si), carbonyl iron (> 99.8 wt.% Fe). Aluminum ingot was melted in an alumund crucible in a vertical resistance furnace. The thermal modes of the melting and pouring was monitored during the whole experiment by a calibrated K-type immersion thermocouple with an accuracy of ± 1.5 °C. Lump-graded silicon was added to the aluminum melt at 800 °C. After dissolving the silicon, powdered iron (<0.5 mm), obtained by grinding drops in a planetary ball mill Fritsch Pulverisette 6 (Germany), was added. Before adding into the melt, the powdered iron was twisted in an aluminum foil of 15 μm thick and compacted into briquettes 10 mm in diameter and 5 mm in height using the hydraulic press Carver 3664 (USA). After the addition of the components, the melt was held for 10 minutes at 850 °C and then manually stirred. Then surface oxides were removed and the melt was purified by dry salt flux addition (47% KCl, 30% NaCl, 23% Na_3AlF_6) in the amount of 0.3 wt.% at 730 °C. The prepared melt was poured at the same temperature into a preheated steel mold with a wall thickness of 30 mm for obtaining samples with a diameter of 20 mm and a length of 100 mm. The mold was coated with a zinc oxide to the thickness about 0.3 mm by a spray gun. Casting regimes for all samples were identical. The chemical composition of the experimental alloys was measured using an ARL ADVANT'X (Thermo Fisher Scientific Inc., USA) X-ray fluorescence spectrometer. Studies of crystallization processes were carried out by the method of differential thermal analysis (DTA) at the standard apparatus "Thermoscan-2" (Russia). Analysis of the samples contained in alumina crucible was carried out in the temperature range 25-1000 °C in an air atmosphere at heating/cooling rates of 5 °C/min. The instrumental error of temperature measurements during DTA tests was estimated as ± 1.2 °C.

The metallographic specimens were cut from the cast samples at a distance of 15 mm from the ingot bottom and prepared according to a standard procedure. The microstructure of the experimental alloys was investigated in the as-cast unetched condition using the Raztek MRX9-D (Russia) digital metallographic microscope. Statistical processing of

metallographic images was carried out using the ImageJ v.1.51 software (NIH, USA). The elemental composition of the phase constituents was determined using a Tescan Vega SBH3 (Czech Republic) scanning electron microscope (SEM) with an energy-dispersive microanalysis system (Oxford Instruments Advanced AZtecEnergy). X-ray diffraction analysis was performed using D8 ADVANCE (BRUKER) with $\text{CuK}\alpha$ radiation ($\lambda = 1.5148 \text{ \AA}$, 40 kV and 40 mA) in the 2θ range (20–85°).

The mechanical properties were examined on standard samples with a working part diameter of 10 mm and a length of 50 mm in the as-cast condition on the universal test machine WDW-100 (China) at room temperature ($\sim 25 \text{ }^\circ\text{C}$) in accordance with ASTM B557 requirements. When investigating the properties and characteristics of experimental alloys, the arithmetic mean and confidence intervals of the measured values were calculated for each series of experiments using the MathCAD v.14.0 software.

The equilibrium phase diagram of Al-Si-Fe system was calculated using Thermo-Calc software with the Al-Alloys Database v5.1 (TTAL5).

3. Results and Discussion

Reportedly [28], phases (Si), Al_3Fe , $\text{Al}_3\text{Fe}_2\text{Si}$ (αAlFeSi) and Al_3FeSi (βAlFeSi), that can take part in various non-variant reactions, are in the equilibrium with the aluminum solid solution. According to the polythermal section of the Al-Si-Fe system calculated for 15 wt.% silicon (Fig. 1), the $\alpha\text{-Al}$, primary silicon and $\beta\text{-Al}_3\text{FeSi}$ phases coexist at the equilibrium conditions below $575 \text{ }^\circ\text{C}$ in the range of iron concentrations from 0 to 2 wt.%. This is in good agreement with the theoretical and experimental data reported in [29] for the Al-Si-Fe system at a fixed iron content of 2 wt.%, which showed the presence of the same phases under these conditions. The isothermal section of the aluminum angle of the Al-Si-Fe phase diagram at $800 \text{ }^\circ\text{C}$ (Fig. 2) shows that for the equilibrium conditions the formation of binary Al_3Fe intermetallics in the Al-15% Si alloy is possible only at iron concentrations exceeding 25 wt.%. At $25 \text{ }^\circ\text{C}$, the three-phase region of coexistence of $\alpha\text{-Al}$, Si and $\beta\text{-Al}_3\text{FeSi}$ occupies the largest part of Al-rich corner including concentration range considered in this work (Fig. 3). At the same time, the presence of various binary and ternary phases, including non-equilibrium ones, is possible in the structure of real industrial alloys at higher cooling rates during crystallization.

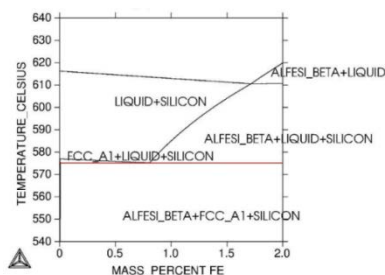


Fig. 1. Calculated polythermal section of Al-Si-Fe phase diagram at constant silicon content equal to 15 wt.% (fragment in the iron concentration range 0–2 wt.%)

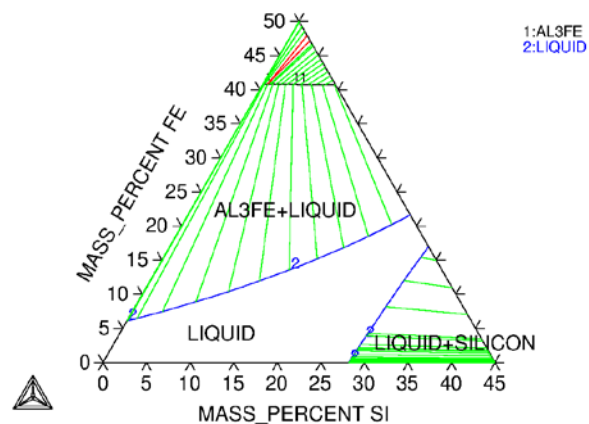


Fig. 2. Calculated isothermal section of Al-Si-Fe phase diagram at $800 \text{ }^\circ\text{C}$ (Al-rich corner)

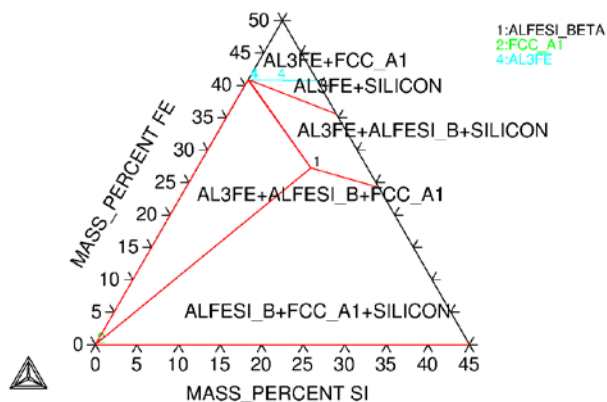


Fig. 3. Calculated isothermal section of Al-Si-Fe phase diagram at $25 \text{ }^\circ\text{C}$ (Al-rich corner)

Fig. 4 shows the microstructures of as-cast samples of the Al-15% Si alloy, containing an iron impurity in different concentrations. Phase constituents, which corresponds to the results of phase diagram calculation, has been metallographically detected in the cast structure of the experimental alloys. In the Al-15% Si-0.3% Fe alloy (Fig. 4 a, b), silicon is released as a block-like or polyhedral crystals having an average size of $18 \mu\text{m}$. With an increase in the iron content to 1.1 wt.%, an increase in the average size of primary Si to $41 \mu\text{m}$ is observed, and at 2 wt.% Fe, a decrease to $17 \mu\text{m}$. The quantitative parameters of the primary Si particles are given in Table 1. In the microstructure of alloys with 2 wt.% iron the needle-like primary crystals of the β -phase clearly appear on the background of the eutectic; its average length is $190 \mu\text{m}$ and maximum length is $425 \mu\text{m}$ (Fig. 4 e, f). Differences in the eutectic structure of alloys with various iron concentrations can be associated with the change in the eutectic crystallization interval, the increase of which leads to the eutectic coarsening.

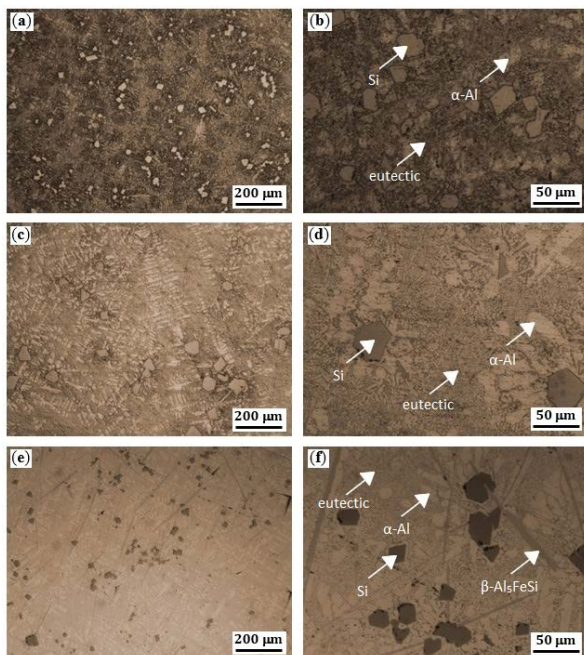


Fig. 4. Microstructure of Al-15% Si alloy with different iron content: 0.3 wt.% (a, b); 1.1 wt.% (c,d); 2.0 wt.% (e, f)

Table 1.

Quantitative parameters of primary silicon particles in Al-15 % Si alloys with different iron content

Parameter	Iron content, wt.%		
	0.3	1.1	2.0
Average size, μm	18	41	17
Maximum size, μm	40	61	35
Total area, %	4.1	3.4	3.6

To assess the elemental composition of the iron-containing phases, an EDX analysis was performed on example of an Al-15% Si alloy with 2 wt.% iron. Fig. 5 demonstrate an SEM image showing needles (platelets) of iron-containing phase and primary silicon crystals against the background of eutectic and α -Al solid solution. The elemental composition at different points is shown in Table 2. Needle-like inclusions containing 16.38 wt.% Si and 24.41 wt.% Fe can be identified as β -Al₃FeSi (composition interval 13-16 wt.% Si and 23-26 wt.% Fe, as reported in [30]).

Table 2.

Elements distribution in phase constituents of Al-15% Si-2% Fe alloy

Point (Fig. 5)	Elements content, wt.% / at.%			Suggested phase
	Al	Si	Fe	
1	59.21/68.26	16.38/18.14	24.41/13.6	β -Al ₃ FeSi
2	1.19/1.24	98.81/98.76	0	Primary silicon
3	97.99/98.17	1.8/1.73	0.21/0.1	α -Al solid solution
4	79.5/80.16	20.46/19.82	0.04/0.02	Eutectic (α -Al + Si)

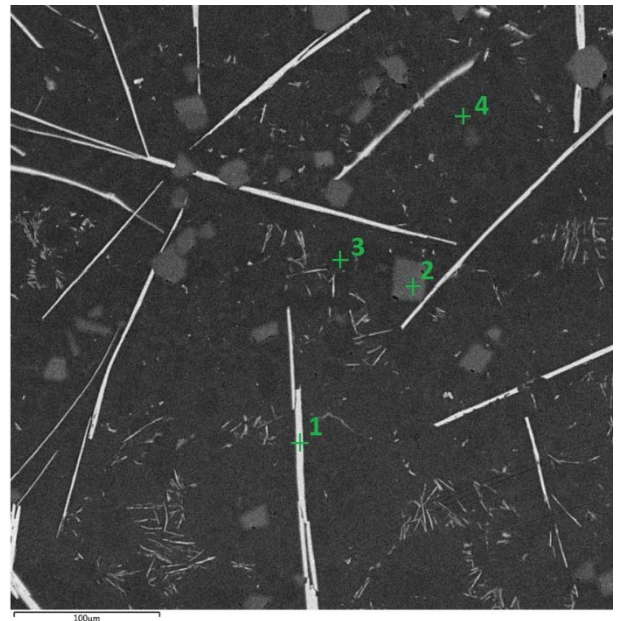


Fig. 5. SEM image of microstructure of Al-15% Si-2% Fe alloy and points of elemental analysis

The presence of β -Al₃FeSi phase is also confirmed by the results of the XRD analysis (Fig. 6). Phase identification according to the ICDD PDF-2 database indicates that the observed phase have a monoclinic crystal structure with lattice parameters $a=b=0.612$ nm, $c=4.15$ nm, and $\beta=91^\circ$, which is corresponds to the work [31].

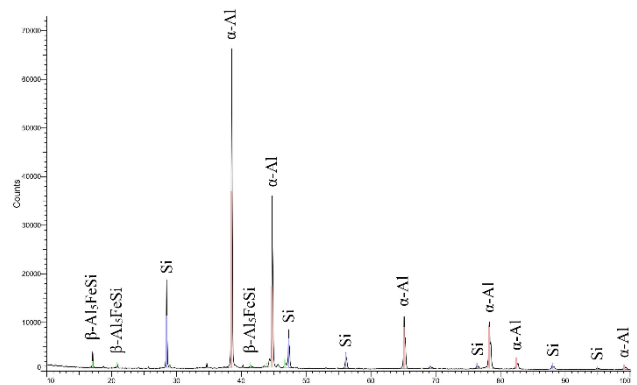


Fig. 6. XRD pattern of Al-15% Si-2% Fe alloy

It was found experimentally that increase of the iron amount up to 1.1 wt.% reduces the alloy liquidus temperature (Table 3). However, with the increase of iron up to 2.0 wt.%, the liquidus temperature becomes higher than at 1.1 wt.% Fe, but it remains significantly lower than that of the Al-15% Si-0.3% Fe alloy. The tendency for a decrease in the liquidus temperature at 1.1 wt.% is consistent with equilibrium calculations in Thermo-Calc, which predict values of 615, 612, and 619 °C at 0.3 wt.%, 1.1 wt.% and 2.0 wt.% Fe, respectively. The solidus temperature at 1.1 wt.% Fe is slightly lower than that of the initial alloy, and at 2 wt.% Fe – is

higher. The presence of iron also increases the time of eutectic crystallization. Along with this, the increase is not proportional to the increase of the iron content: at 1.1 wt.% Fe it is greater than that of the alloy with 0.3 wt.% Fe, and at 2 wt.% Fe decreases again, but insignificantly.

Table 3.

Crystallization parameters of Al-15 % Si alloy with different iron content

Parameter	Iron content, wt.%		
	0.3	1.1	2.0
Liquidus temperature, °C	651	619	630
Solidus temperature, °C	575	572	584
Time of eutectic crystallization, min	6.2	7.6	7.2

The observed facts can be related to the following. In the Al-15% Si-0.3% Fe alloy, the iron-bearing phases are in the structure of eutectic ($\beta + \alpha\text{-Al} + \text{Si}$) [32]. With increase of iron content to 1.1 wt.%, the eutectic volume fraction increases [28], as well as the presence of primary crystals of the $\beta\text{-Al}_5\text{FeSi}$ phase is noted (see Fig. 4 c, d). In a complex, this leads to increase in the eutectic crystallization time and to decrease in the liquidus temperature of the alloy. Apparently, a longer eutectic crystallization time can contribute to the intensification of liquation processes and to the formation of a pronounced dendritic structure. At 2 wt.% Fe, large crystals of $\beta\text{-Al}_5\text{FeSi}$ phase are observed against the backdrop of some refinement of the primary silicon crystals and decrease in the amount of eutectic, which contributes to decrease in the eutectic crystallization time from 7.6 s to 7.2 s and increase in the liquidus temperature as compared to the alloy containing 1.1 wt.% Fe. Presumably [33], a decrease in the size of silicon inclusions at 2 wt.% Fe may be caused by the fact that the ternary iron-containing intermetallic compounds $\delta\text{-Al}_4\text{FeSi}_2$ and $\beta\text{-Al}_5\text{FeSi}$ can act as substrates of primary silicon crystallization in hypereutectic aluminum-silicon alloys.

Dependence of the critical iron concentration (from the standpoint of its influence on casting and mechanical properties) on the silicon content in aluminum-silicon alloys was proposed by J. Taylor [34]:

$$[\text{Fe}]_{crit} \approx 0.075 \cdot [\text{Si}, \text{wt. \%}] - 0.05 \quad (1)$$

It is obvious that an increase in the silicon concentration in the alloy will lead to an increase in the critical iron concentration, allowing to use the alloys with a higher iron content in practice. Exceedance of the critical iron concentration leads to a sharp deterioration of mechanical properties of castings due to the formation of large intermetallic inclusions of β -phase having unfavorable shape. This is due to the fact that with an increase of iron impurity content, the total amount and average sizes of iron-containing intermetallics increase, which leads to an extreme drop in ductility due to the transition to brittle fracture [35]. According to the equation (1), the calculated value of critical iron content for the Al-15% Si alloy is ~ 1.08 wt.%.

Mechanical properties of the Al-15% Si alloy significantly decrease with an increase in the iron content above the critical value (Fig. 7). With a content of 2 wt.% Fe, the tensile strength decreases on the average by 1.4 times, and the ductility by 2.6

times compared with the alloy with 0.3 wt.% Fe. At the same time, the presence of iron impurity at the amount of 1.1 wt.% leads to a relatively small decrease in the ductility of the experimental alloys. Such nature of the change in properties can be explained by the fact that with an increase in the iron content from 1.1 to 2.0 wt.%, large and brittle lamellar precipitates of the $\beta\text{-Al}_5\text{FeSi}$ phase appear, which have a relatively low bond strength with the aluminum matrix and easily breaks under load.

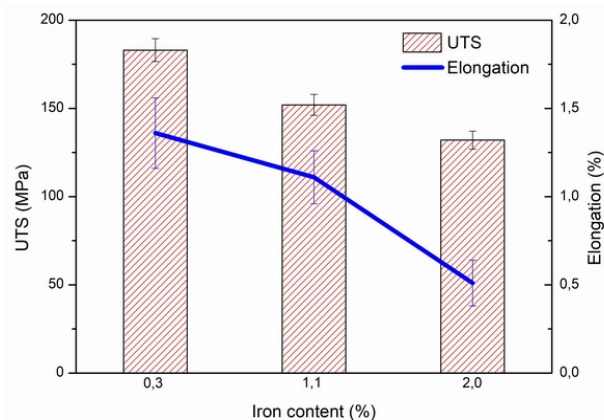


Fig. 7. Ultimate tensile strength (MPa) and elongation (%) of Al-15% Si alloy with different iron content (0.3; 1.1; 2.0 wt.%)

The obtained results confirm that secondary hypereutectic aluminum alloys with an iron content of about 1 wt.% can be successfully used in the manufacture of cast products, because satisfactorily high values of tensile strength and ductility remain at this concentration. Thus, from the point of view of recyclability, hypereutectic Al-Si alloys allow a higher content of iron impurity in comparison with hypoeutectic ones. In the case of exceeding the critical concentration, as the practical experience of foundries shows, it is advisable to use casting technologies that provide high cooling rates of the melt in the mold. The high cooling rate positively affects the structure of the alloys, changing the morphology of the iron-containing phases and allows to produce high-quality castings with a sufficiently high mechanical properties.

5. Conclusion

In this work, the crystallization behavior and microstructure evolution of Al-15%Si-XFe alloys (where X = 0.3, 1.1 and 2 wt.% Fe) was studied. The eutectic crystallization time increases from 6.2 to 7.6 s with an increase in the iron impurity content in the Al-15% Si alloy from 0.3 wt.% to 1.1 wt.%. At that, the amount of the eutectic phase increases, which leads to a decrease in the liquidus temperature of the alloy from 651 to 619 °C. A subsequent increase in the iron concentration up to 2.0 wt.% leads to a slight decrease in the eutectic crystallization time to 7.2 s and an increase in the liquidus temperature to 630 °C. According to thermodynamic calculations, the primary silicon and the $\beta\text{-Al}_5\text{FeSi}$ phase coexist in the structure of the Al-15% Si alloys at a temperature below 575 °C in the range of iron concentrations

from 0 to 2 wt.% in equilibrium conditions; meanwhile, in the real alloys structure, the primary crystals of the β -phase were metallographically detected only in the alloys containing 1.1 wt.% and 2 wt.% of iron impurity. An increase in the iron content in the alloy from 0.3 to 1.1 wt.% leads to a decrease in tensile strength from 183 to 152 MPa and elongation from 1.36 to 1.11%, respectively. Further increase of the iron content up to 2 wt.% significantly reduces the tensile strength (to 132 MPa) and ductility (to 0.51%) of the Al-15% Si alloy due to the formation of large intermetallic inclusions of β -Al₃FeSi phase having large sizes (average length is 190 μ m and maximum length is 425 μ m) and unfavorable shape.

Acknowledgements

This work was carried out with the support of the Ministry of Science and Higher Education of the Russian Federation (project code 0718-2020-0030).

References

- [1] Zhao, Y., Du, W., Koe, B., Connolley, T., Irvine, S., Allan, P. K., Schlepütz, C. M., Zhang, W., Wang, F. & Eskin, D. G. (2018). 3D Characterisation of the Fe-Rich Intermetallic Phases in Recycled Al Alloys by Synchrotron X-Ray Microtomography and Skeletonisation. *Scripta Materialia*. 146, 321–326.
- [2] Lu, H., Hou, Z., Ma, M. & Lu, G. (2017). Effect of Fe-Content on the Mechanical Properties of Recycled Al Alloys during Hot Compression. *Metals*. 7, 262
- [3] Zhang, L., Gao, J., Damoah, L.N.W. & Robertson, D.G. (2012). Removal of Iron from Aluminum: a Review. *Mineral Processing and Extractive Metallurgy Review*. 33, 99-157.
- [4] Deev, V.B., Selyanin, I.F., Kutsenko, A.I., Belov, N.A. & Ponomareva, K.V. (2015). Promising Resource Saving Technology for Processing Melts During Production of Cast Aluminum Alloys. *Metallurgist*. 58(11-12), 1123-1127.
- [5] Sweet, L., Zhu, S. M., Gao, S. X., Taylor, J. A. & Easton, M. A. (2011). The Effect of Iron Content on the Iron-Containing Intermetallic Phases in A Cast 6060 Aluminum Alloy. *Metallurgical and Materials Transactions A*. 42, 1737-1749.
- [6] Tenekedjiev, N & Gruzleski, J.E. (1990). Hypereutectic Aluminium-Silicon Casting Alloys – A Review. *Cast Metals*. 3(2), 96-105.
- [7] Abouei, V., Shabestari, S.G. & Saghafian, H. (2010). Dry Sliding Wear Behaviour of Hypereutectic Al–Si Piston Alloys Containing Iron-Rich Intermetallics. *Materials Characterization*. 61, 1089-1096.
- [8] Darvishi, A., Maleki, A., Atabaki, M.M. & Zargami, M. (2010). The Mutual Effect of Iron and Manganese on Microstructure and Mechanical Properties of Aluminium-Silicon Alloy. *Metallurgija-Journal of Metallurgy*. 16(1), 11-24.
- [9] Šćepanović, J., Asanović, V., Radonjić, D., Vukšanović, D., Herenda, S., Korać, F. & Bikić, F. (2019). Mechanical properties and corrosion behaviour of Al–Si alloys for IC engine. *Journal of the Serbian Chemical Society*. 84(5), 503-516.
- [10] Otani, L.B., Soyama, J., Zepon, G., Silva, A.C., Kiminami, C.S., Botta, W.J. & Bolfarini, C. (2017). Predicting the Formation of Intermetallic Phases in the Al-Si-Fe System with Mn Additions. *Journal of Phase Equilibria and Diffusion*. 38, 298-304.
- [11] Dinnis, C.M., Taylor, J.A. & Dahle, A.K. (2005). As-Cast Morphology of Iron-Intermetallics in Al–Si Foundry Alloys. *Scripta Materialia*. 53, 955-958.
- [12] Mikołajczak, P. & Ratke, L. (2015). Three Dimensional Morphology of β -Al₃FeSi Intermetallics in AlSi Alloys. *Archives of Foundry Engineering*. 15(1), 47-50.
- [13] Hatch, J.E. (1984). *Aluminum: Properties and Physical Metallurgy*. (2nd ed.). Metals Park (OH): American Society for Metals.
- [14] Mahta, M., Emamy, M., Cao, X. & Campbell, J. (2008). Overview of β -Al₃FeSi phase in Al-Si alloys. In: L. V. Olivante (Ed.), *Materials Science Research Trends*. 251-271. Nova Science Publishers: New York.
- [15] Lu, S., Wu, S., Lin, C. & An, P. (2014). Microstructure and Properties of In Situ Si and Fe-rich Particles Reinforced Al Matrix Composites Assisted with Ultrasonic Vibration. *Acta Metallurgica Sinica (English Letters)*. 27, 862-868.
- [16] Władysławski, R., Kozun, A. & Pacyniak, T. (2016). Effect of Casting Die Cooling On Solidification Process and Microstructure of Hypereutectic Al-Si Alloy. *Archives of Foundry Engineering*. 16(4), 175-180.
- [17] Murali, S., Raman K. S. & Murthy, K. S. S. (1992). Effect of Magnesium, Iron (Impurity) and Solidification Rates on the Fracture Toughness of Al-7Si-0.3Mg Casting Alloy. *Materials Science and Engineering: A*. 151, 1-10.
- [18] Hren, I., Svobodova, J. & Michna, Š. (2018). Influence of Al₃FeSi Phases on the Cracking of Castings at Al-Si Alloys. *Archives of Foundry Engineering*. 18(4), 120-124.
- [19] Taghaddos, E., Hejazi, M. M., Taghiabadi, R. & Shabestari, S. G. (2009). Effect of Iron-Intermetallics on the Fluidity of 413 Aluminum Alloy. *Journal of Alloys and Compounds*. 468, 539-545.
- [20] Jorstad, J. & Apelian, D. (2009). Hypereutectic Al-Si Alloys: Practical Casting Considerations. *International Journal of Metallcasting*. 3, 13-36.
- [21] Prusov, E. S., Panfilov A. A. & Kechin V. A. (2017). Role of Powder Precursors in Production of Composite Alloys Using Liquid-Phase Methods. *Russian Journal of Non-Ferrous Metals*. 58, 308-316.
- [22] Khalifa, W., El-Hadad, S. & Tsunekawa, Y. (2013). Microstructure and Wear Behavior of Solidification Sonoprocessed B390 Hypereutectic Al-Si Alloy. *Metallurgical and Materials Transactions A*. 44, 5817-5824.
- [23] Wang, Q., Zhang, S., Zhang, Z., Yan, X. & Geng, H. (2013). Study of Melt Thermal-Rate Treatment and Low-Temperature Pouring on Al-15%Si Alloy. *JOM*. 65, 958-966.
- [24] Wieszala, R. & Piatkowski, J. (2017). Selected Tribological Properties of A390.0 Alloy. *Archives of Foundry Engineering*. 17(4), 175-178.
- [25] Bidmeshki, C., Abouei, V., Saghafian, H., Shabestari, S.G. & Noghani, M.T. (2016). Effect of Mn addition on Fe-rich intermetallics morphology and dry sliding wear investigation

- of hypereutectic Al-17.5%Si alloys. *Journal of Materials Research and Technology*. 5(3) 250-258.
- [26] Lin, C., Wu, S., Lü, S., Wu, H. & Chen, H. (2019). Influence of high pressure and manganese addition on Fe-rich phases and mechanical properties of hypereutectic Al-Si alloy with rheo-squeeze casting. *Transactions of Nonferrous Metals Society of China*. 29(2), 253-262.
- [27] Ivanov, Y.F., Alsaraeva, K.V., Gromov, V.E., Popova, N.A. & Konovalov, S.V. (2015). Fatigue life of silumin treated with a high-intensity pulsed electron beam. *Journal of Surface Investigation*. 9, 1056-1059.
- [28] Belov, N. A., Aksenov, A. A. & Eskin, D. G. (2002). *Iron in Aluminum Alloys: Impurity and Alloying Element*. London: Taylor&Francis.
- [29] Liu, Z.K & Chang, Y.A. (1999). Thermodynamic Assessment of the Al-Fe-Si System. *Metallurgical and Materials Transactions A*. 30A, 1081-1095.
- [30] Mrówka-Nowotnik, G., Sieniawski, J. & Wierzbińska, M. (2007). Intermetallic phase particles in 6082 aluminium alloy. *Archives of Materials Science and Engineering*. 28(2), 69-76.
- [31] Mondolfo, L.F. (1976). *Aluminium Alloys: Structure and Properties*. London: Butterworth.
- [32] Mbuya, T.O., Odera, B.O. & Ng'ang'a S.P. (2003). Influence of iron on castability and properties of aluminium silicon alloys: literature review. *International Journal of Cast Metals Research*. 16(5), 451-465.
- [33] Suarez, M.A., Figueroa, I., Cruz, A., Hernandez, A. & Chavez J. F. (2012). Study of the Al-Si-X System by Different Cooling Rates and Heat Treatment. *Materials Research*. 15, 763-769.
- [34] Taylor J. A. (2012). Iron-Containing Intermetallic Phases in Al-Si Based Casting Alloys. *Procedia Materials Science*. 1, 19-33.
- [35] Taylor J.A. (1997) *The Role of Iron in the Formation of Porosity in Al-Si-Cu Alloy Castings, PhD Thesis*. Brisbane: University of Queensland.